0026-895X/06/7004-1174–1183$20.00
MOLECULAR PHARMACOLOGY
Copyright © 2006 The American Society for Pharmacology and Experimental Therapeutics
Mol Pharmacol 70:1174–1183, 2006

Vol. 70, No. 4
21741/3139169
Printed in U.S.A.

Caveolin-1 Regulates Store-Operated Ca^{2+} Influx by Binding of Its Scaffolding Domain to Transient Receptor Potential Channel-1 in Endothelial Cells

Angela M. Kwiatek, Richard D. Minshall, David R. Cool, Randal A. Skidgel, Asrar B. Malik, and Chinnaswamy Tiruppathi

Department of Pharmacology and Center for Lung and Vascular Biology, College of Medicine, University of Illinois at Chicago, Chicago, Illinois (A.M.K., R.D.M., R.A.S., A.B.M., C.T.); and Department of Pharmacology/Toxicology, Boonshoft School of Medicine, Wright State, University, Dayton, Ohio (D.R.C.)

Received December 15, 2005; accepted July 5, 2006

ABSTRACT

Caveolin-1 associates with store-operated cation channels (SOC) in endothelial cells. We examined the role of the caveolin-1 scaffolding domain (CSD) in regulating the SOC [i.e., transient receptor potential channel-1 (TRPC1)] in human pulmonary artery endothelial cells (HPAECs). We used the cell-permeant antennapedia (AP)-conjugated CSD peptide, which competes for protein binding partners with caveolin-1, to assess the interactions of caveolin-1 with TRPC1 and its consequences on thrombin-induced Ca^{2+} influx. We observed that AP-CSD peptide markedly reduced thrombin-induced Ca^{2+} influx via SOC in HPAECs in contrast to control peptide. AP-CSD also suppressed thapsigargin-induced Ca^{2+} influx. Streptavidin-bead pull-down assay indicated strong binding of biotin-labeled AP-CSD peptide to TRPC1. Immunoprecipitation studies demonstrated an interaction between endogenous TRPC1 and ectopically expressed hemagglutinin-tagged CSD. Analysis of the deduced TRPC1 amino acid sequence revealed the presence of CSD binding consensus sequence in the TRPC1 C terminus. We also observed that an AP-TRPC1 peptide containing the CSD binding sequence markedly reduced the thrombin-induced Ca^{2+} influx. We identified the interaction between biotin-labeled AP-TRPC1 C terminus peptide and caveolin-1. Thus, these results demonstrate a crucial role of caveolin-1 scaffolding domain interaction with TRPC1 in regulating Ca^{2+} influx via SOC.

Proinflammatory mediators such as thrombin, histamine, and reactive oxygen species increase vascular permeability in part by activating Ca^{2+}-sensitive signaling pathways (Tiruppathi et al., 2003). We showed that Ca^{2+} entry through plasma membrane cation channels activated by Ca^{2+}-stored depletion is a critical determinant of increased endothelial permeability (Sandoval et al., 2001a,b; Tiruppathi et al., 2002). We also have shown that activation of endothelial cell surface protease-activated receptor-1 by thrombin caused a rapid and transient increase in cytosolic Ca^{2+} concentration ($[Ca^{2+}]_i$) due to the release of stored Ca^{2+} and subsequent Ca^{2+} entry induced by store depletion (Sandoval et al., 2001a). In endothelial cells, the plasma membrane cation channels known as store-operated cation channels (SOCs) contribute to the entry of Ca^{2+} into cells (Nilius and Droogmans, 2001). Several studies have shown the important role the influx of Ca^{2+} through SOCs in vascular endothelial cells (Freichel et al., 2001; Nilius and Droogmans, 2001; Tiruppathi et al., 2002). Studies identified that the mammalian homologs of transient receptor potential (TRP) gene family of channels function as SOCs (Nilius and Droogmans, 2001; Tiruppathi et al., 2003). TRP genes encode a superfamily of proteins with six transmembrane helices that are divided into seven subfamilies: TRPC (canonical or classic), TRPV (vanilloid), TRPM (melastatin), TRPA (ankyrin), TRPML (mucolipin), TRPP (polycystin), and the TRPN (no mechanoreceptor potential C) (Montell et al., 2002; Pedersen et al.,

This work was supported by National Institutes of Health Grants GM58531, P01 HL077806, and T32HL007829.
Article, publication date, and citation information can be found at http://molpharm.aspetjournals.org.
doi:10.1124/mol.105.021741.

ABBREVIATIONS: SOC, store-operated cation channel; Cav-1, caveolin-1; TRP, transient receptor potential; TRPC1, transient receptor potential channel-1; CSD, caveolin-1 scaffolding domain; HPAEC, human pulmonary artery endothelial cell; AP, antennapedia; Ab, antibody; HA, hemagglutinin; ER, endoplasmic reticulum; eNOS, endothelial nitric-oxide synthase; HBSS, Hanks' balanced salt solution; FBS, fetal bovine serum; AM, acetoxymethyl ester; mAb, monoclonal antibody; MS, mass spectrometry; HMEC, human dermal microvessel endothelial cell line; SELDI-TOF, surface-enhanced laser/desorption ionization-time of flight; PAGE, polyacrylamide gel electrophoresis; WT, wild-type; PCR, polymerase chain reaction; IP_3, inositol 1,4,5-trisphosphate.

2005). Members of TRPC subfamily contain 700 to 1000 amino acids and 7 isoforms (TRPC1 to -7) that are expressed in mammalian cells. Mammalian TRPCs are grouped into four subfamilies. One group consists of TRPC4 and TRPC5. Their activation is dependent on Ca^{2+}-stored depletion and they have high Ca^{2+} selectivity, as assessed by their sensitivity to La^{3+} (Nilius and Droogmans, 2001). TRPC4 and TRPC5 are activated by G protein-coupled receptors and receptor tyrosine kinases coupled to phospholipase C. In the second group, TRPC1 is closely related to TRPC4 and TRPC5; although it forms SOCs, it is a less selective Ca^{2+} channel. Third, TRPC3, TRPC6, and TRPC7 form store-independent nonselective cation channels activated by diacylglycerol (Dietrich et al., 2003); however, a store-dependent activation mechanism has been described for human TRPC3 (Liu et al., 2000). In the last subfamily, TRPC2 function is unclear, and it is believed to be a pseudogene in humans (Montell et al., 2002).

TRPC1 has been shown to be localized within cholesterol-rich invaginations of the cell membrane called caveolae (Brazer et al., 2003). Caveolae are coated with a 22-kDa protein, caveolin-1 (Cav-1). Studies have shown that Ca^{2+} influx occurs via caveolae in response to ER-stored Ca^{2+} depletion in endothelial cells (Isshiki et al., 2002). Furthermore, Cav-1 seems to be necessary for anchoring TRPC1 to caveolae (Lockwich et al., 2000), but it is unclear how this interaction regulates TRPC1 function in endothelial cells. Cav-1 scaffolding domain (CSD), located between residues 82 and 101 of Cav-1, binds many signaling molecules, including endothelial nitric-oxide synthase (eNOS), Src-like kinases, Ha-Ras, and heterotrimeric G-proteins (Schlegel and Lisanti, 2001). Binding of these proteins to CSD in many cases negatively regulates their function (Drab et al., 2001). For example, binding of eNOS to CSD holds eNOS in an inactive state. Bucci et al. (2000) observed the inhibition of acetylcholine-induced NO production and vasodilation in bovine aortic endothelial cells by cell membrane-permeable CSD peptide. Moreover, acute vascular inflammation in mice was prevented by systemic administration of cell-permeable CSD-peptide. Another study demonstrated that CSD peptide administration markedly reduced platelet-activating factor-induced increase in microvessel permeability in rats (Zhu et al., 2004). Recently, Bernatchez et al. (2005) showed that CSD sequence containing the residues 89 to 95 is sufficient to inhibit eNOS activity and NO release from endothelial cells. Because Ca^{2+} signaling in the endothelium is critical in regulating endothelial permeability, we addressed the possible role of CSD in the TRPC1-mediated Ca^{2+} influx in endothelial cells. We observed that cell-permeable CSD sequence markedly reduced ER-stored Ca^{2+} release and the Ca^{2+} release-activated Ca^{2+} influx in response to thrombin challenge of endothelial cells. This response was dependent on the specific interaction between CSD and TRPC1. Analysis of the deduced TRPC1 amino acid sequence revealed the presence of CSD binding consensus sequence in TRPC1 C terminus. A synthetic peptide corresponding to CSD binding consensus sequence present in the C terminus of TRPC1 was shown to inhibit the thrombin-induced Ca^{2+} influx in endothelial cells.

Materials and Methods

Materials. Human α-thrombin was obtained from Enzyme Research Laboratories (South Bend, IN). Endothelial growth medium was obtained from Cambrex Bio Science (Walkersville, MD). Hanks' balanced salt solution (HBSS) and trypsin were from Invitrogen (Carlsbad, CA). Fetal bovine serum (FBS) was from HyClone (Logan, UT). Fura 2-AM was purchased from Molecular Probes (Eugene, OR). Anti-HA monoclonal antibody (mAb) was obtained from Sigma (St. Louis, MO). Anti-cSrc monoclonal and anti-TRPC1 polyclonal antibodies were obtained from Santa Cruz Biotechnology (Santa Cruz, CA). Streptavidin cross-linked agarose and streptavidin-conjugated rhodamine were obtained from Pierce Biotechnology (Rockford, IL). Peptides were synthesized at a commercial facility (bioWORLD, Dublin, OH). CSD sequence (amino acids 82–101, DGIWKASFTTFTVTKYWFYR) was synthesized as a fusion peptide to the C terminus of the antennapedia (AP) internalization sequence (RQIKIWFQNRRMKWKK) (Bucci et al., 2000). The cell-permeable AP sequence was used as a control peptide. The C-terminal TRPC1 peptide [amino acids 781–789 (FRTSKYAMF)] was synthesized as a fusion peptide to the C terminus of the AP internalization sequence. All peptides were synthesized as C-terminal amide, and N terminus was labeled with biotin. Peptide purity and amino acid sequence were determined by high-performance liquid chromatography and MS, respectively. Peptides used in this study were 98% pure.

Cell Culture. Human pulmonary artery endothelial cells (HPAECs) were grown in endothelial growth medium supplemented with 10% FBS. Cells were cultured on tissue culture dishes coated with 0.1% gelatin. HPAECs used in the experiments were between five and seven passages. Human dermal microvessel endothelial cell line (HMEC) was grown as described previously (Ellis et al., 1999).

Cell Volume Measurement. HPAECs grown in 100-mm culture dishes were incubated with 1% FBS medium in the presence of 1 μCi/ml [^{3}H]D-mannitol (D-[1-^{3}H(*N*)]-mannitol) for 4 h at 37°C to reach equilibrium. After incubation, cells were placed on ice and washed two times with HBSS. Cells were lysed with lysis buffer (50 mM Tris-HCl buffer, pH 7.4, containing 0.5% sodium deoxycholate, 1% Triton X-100) for 1 h at 4°C. The radioactivity associated with the cell lysate was determined using liquid scintillation counter. HPAECs grown in culture dishes were trypsinized, and cell numbers were counted. Cell volume was determined using the equilibrium [^{3}H]D-mannitol uptake and cell numbers. Based on these measurements, we obtained cell volume of 2.5 μl/10^6 cells.

Measurement of Peptide Concentration inside HPAECs. Cell-permeable peptides reached inside HPAECs were determined using surface-enhanced laser/desorption ionization-time of flight mass spectrometry (SELDI-TOF MS) as described previously (Cool and Hardiman, 2004; Hardiman et al., 2005). HPAECs grown to confluence on 100-mm culture dishes were incubated with 1% FBS containing medium in the presence or absence of the AP or AP-CSD peptide for 4 h at 37°C. After the incubation, cells were placed on ice and washed two times with acid buffer (50 mM acetate buffer, pH 4.5, containing 0.15 M NaCl). Then cells were washed two times with HBSS, scraped, and pelleted by centrifugation at 500*g* for 10 min. The cell pellet (containing $\sim 1.6 \times 10^6$ cells) was homogenized in 20 μl of 0.1 N HCl and centrifuged for 5 min at 13,000 rpm to remove cell debris. The supernatant was applied on the Ciphergen WCX2 (weak cation exchange) ProteinChip. The sample spots were allowed to nearly dry (still damp) and then were rinsed individually with 5 μl of water to remove unwanted and unbound debris. The energy-absorbing molecule matrix (1 μl) α-cyano-4-hydroxy cinnamic acid in 50% acetonitrile and 0.1% trifluoroacetic acid was added to each spot to aide in the ionization of peptides. The ProteinChips were placed into the Ciphergen SELDI-TOF ProteinChip Array for analysis. A spot-and-chip protocol was designed to take 10 transients at every 5 sites beginning at 20 and ending at 80 (each spot has 100 possible sites). The laser intensity was set to 155 for each sample with two warming shots at 160 intensity. The Ciphergen version 3.2 software

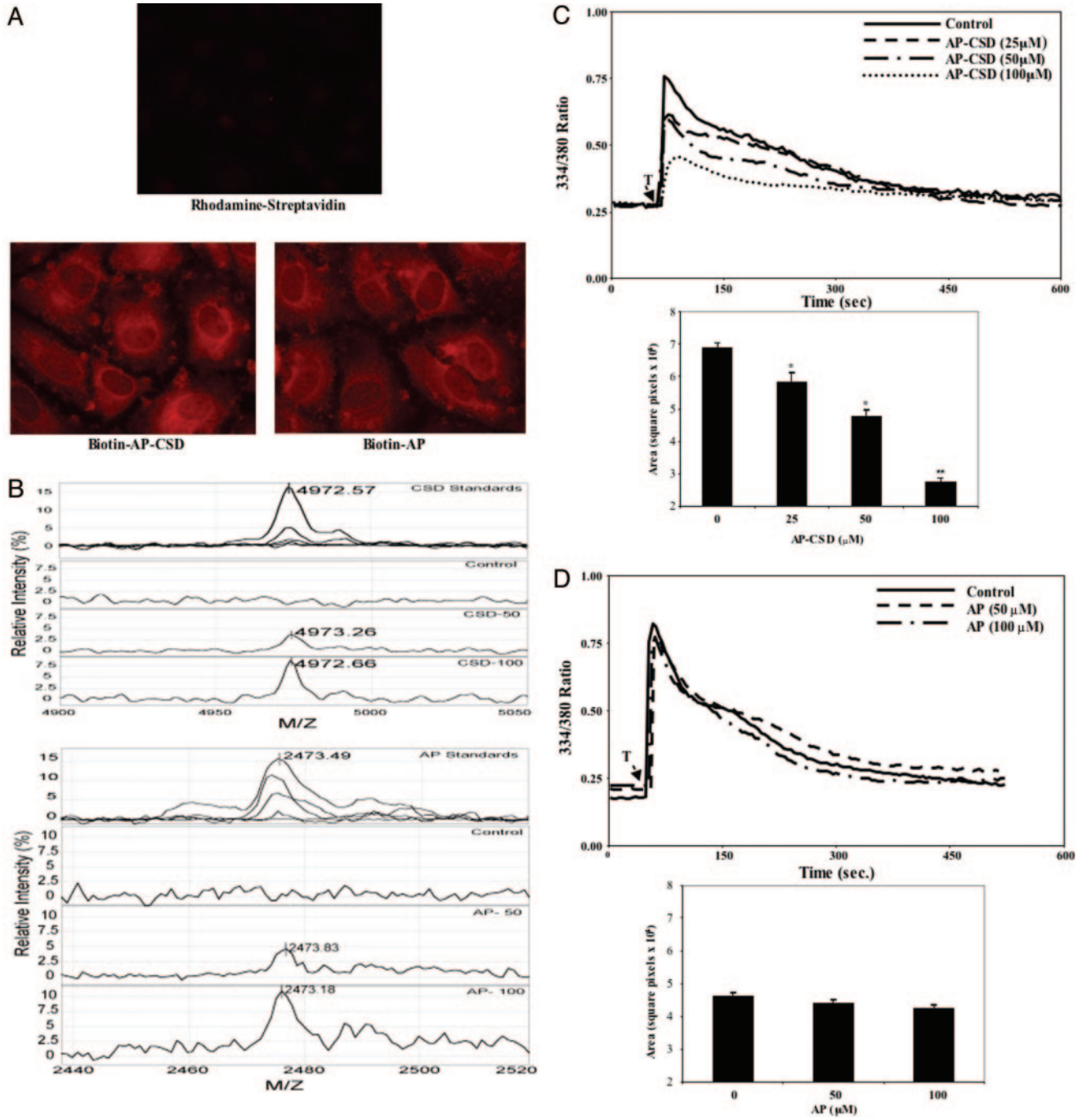

Fig. 1. A, internalization of AP or AP-CSD peptide in HPAECs. HPAECs grown to confluence on glass coverslips were washed and incubated with 1% FBS medium containing either AP (25 μM) or AP-CSD (25 μM) for 4 h at 37°C. After incubation, cells were washed three times on ice with acid buffer (50 mM acetate buffer, pH 4.5, containing 0.5 M NaCl) to remove cell surface-bound peptides, fixed with 2% paraformaldehyde and permeabilized with 0.1% Triton X-100 (Bucci et al., 2000). Cells were then stained with rhodamine-labeled streptavidin and images were obtained from a Zeiss Axiovert 25 fluorescent microscope. B, SELDI-TOF mass spectrometric analysis of peptides associated with HPAECs. HPAECs were incubated with either CSD (AP-CSD) or AP peptides for 4 h at 37°C. After this incubation, cell pellets obtained were used for SELDI-TOF mass spectrometric analysis as described under *Materials and Methods*. The molecular masses of CSD (4972.57 Da) and AP (2473.49 Da) were identified using the synthetic peptides. A representative analysis is shown. Control, cells not exposed to either CSD or AP peptide; CSD-50, cells incubated with 50 μM CSD; CSD-100, cells incubated with 100 μM CSD; AP-50, cells incubated with 50 μM AP; AP-100, cells incubated with 100 μM AP. m/z indicates mass/charge and is represented as daltons in the spectra. The relative concentrations of peptides present inside the cells were calculated using spectra from different concentrations of peptides as described under *Materials and Methods*. The experiment was repeated three times, and the results are summarized in Table 1. C, top, CSD peptide inhibits thrombin-induced increase in intracellular Ca^{2+} in HPAECs. HPAECs grown to confluence were incubated with the indicated concentrations of AP-CSD peptide and then used for measuring cytosolic Ca^{2+} (see details under *Materials and Methods*). Cells were stimulated with thrombin in the presence of nominal Ca^{2+} (1.26 mM) in the extracellular medium. Arrow indicates the time at which cells were stimulated with thrombin (50 nM). Results shown are representative of four experiments. In each experiment, 30 to 50 cells were selected to measure change in $[Ca^{2+}]_i$. The relative area of peak increase in $[Ca^{2+}]_i$ after thrombin-stimulation in control and AP-CSD peptide exposed cells was compared (bottom). *, $p < 0.01$; **, $p < 0.005$. D, top, the experiment was carried out as described in C, except that cells were incubated with AP peptide. Results shown are representative of four experiments. The relative area of peak increase in $[Ca^{2+}]_i$ after thrombin-stimulation in control and AP peptide exposed cells were compared (bottom).

was used to analyze each spectrum for the peptides of choice. The CSD and AP peptides were suspended in 0.1 N HCl to a concentration of 1 mM, and serial 1:5 dilutions were analyzed for both peptides. Integrated area under each observed ion peak was plotted against the concentration of peptide, and the linear regression formula was determined. The concentrations of the peptides in the cell lysate samples were determined using this formula.

Cytosolic Ca^{2+} Measurement. Increase in cytosolic Ca^{2+} ($[Ca^{2+}]_i$) was measured using the Ca^{2+}-sensitive fluorescent dye Fura 2-AM (Tiruppathi et al., 2002). Cells were grown to confluence on 0.1% gelatin-coated 25-mm glass coverslips to confluence. Cells were incubated with or without peptides in 1% FBS containing medium for 4 h at 37°C. Cells were washed two times with HBSS and loaded with 3 μM Fura 2-AM for 30 min. Cells were washed again two times with HBSS and then imaged using an Attoflor Ratio Vision digital fluorescence microscopy system (Atto Instruments, Rockville, MD) equipped with a Zeiss Axiovert S 100 inverted microscope (Carl Zeiss Inc., Thornwood, NY) and F-Fluar 40x, 1.3 numerical aperture oil immersion objective. Regions of interest in individual cells were marked and excited at 334 and 380 nm with emission at 520 nm at 5-s intervals. In each experiment, 30 to 50 cells were selected to measure change in $[Ca^{2+}]_i$. The cells were then stimulated with either thrombin or thapsigargin. The area under the curve (the total Ca^{2+} transient peak, ER-stored Ca^{2+} release peak, and influx peak) was quantified using ImageJ version 1.31 program.

Streptavidin-Agarose Beads Affinity Precipitation. Proteins bound to biotin-labeled peptides were precipitated using streptavidin-agarose beads. HPAECs grown to confluence were incubated with either AP-CSD or AP at the indicated concentration for 4 h at 37°C. After incubation, cells were placed on ice and washed two times with HBSS. Cells were lysed with lysis buffer (50 mM Tris-HCl buffer, pH 7.4, containing 0.5% sodium deoxycholate, 1% Triton X-100, 1 mM orthovanadate, and protease inhibitors) for 1 h at 4°C. The lysates were centrifuged at 60,000*g* for 30 min. The obtained supernatant was mixed with streptavidin-agarose beads and incubated for 1 h at 4°C with shaking. After this treatment, the suspension was centrifuged at 5000*g* for 10 min. The supernatant was discarded, and the beads were washed three times with 50 mM Tris-HCl buffer, pH 7.4, containing 1 M NaCl and 0.1% Triton X-100. After removing the supernatant from the last wash, SDS-PAGE sample buffer was added to the beads, boiled for 5 min, and centrifuged at 5000*g* for 5 min at 22°C. Proteins present in the supernatant were separated on an SDS-PAGE and immunoblotted with the appropriate antibodies.

Preparation of Expression Constructs. Myc-TRPC1 cDNA expression construct was prepared as described previously (Paria et al., 2003). Caveolin-1 wild-type (WT-Cav-1) cDNA in pcDNA3.1 expression construct was made as described previously (Minshall et al., 2000). Cav-1-14F mutant was prepared by PCR method using the QuikChange Site Directed Mutagenesis Kit (Stratagene, La Jolla, CA). HA-tagged CSD expression construct was also prepared using PCR method. To generate N-terminal HA-tagged CSD domain, the human wild-type Cav-1 was PCR-amplified using the following primers: forward, 5′-ACAGAATTCGCACACGGCATTTGGAAG-3′; and reverse, 5′-ACAACA*CTCGAG*TTATTAGCGGTAAAACCAG-3′. The resulting DNA fragment (63 base pairs) was subcloned into the 5′-EcoR1 and 3′-XhoI restriction sites (underlined in primers) of pcDNA3-HA vector. Cav-1-14F mutant and HA-tagged CSD expression constructs sequences were verified by DNA sequencing. These expression constructs were transfected into HMECs using LipofectAMINE Plus reagent in serum-free Dulbecco's modified Eagle's medium as we described previously (Ellis et al., 1999). At 48 h after transfection, cells were used for intracellular Ca^{2+} measurement and immunoprecipitation experiments.

Statistics. Statistical comparisons were made using the two-tailed Student's *t* test. Experimental values were reported as means ± S.E. Differences in mean values were considered significant at $p < 0.05$.

Results

Cell-Permeable CSD Peptide Inhibits Thrombin-Induced Increase in $[Ca^{2+}]_i$. We determined the contribution of CSD in regulating the thrombin-induced increase in $[Ca^{2+}]_i$ in HPAECs. We synthesized the CSD sequence (residues 82–101, DGIWKASFTTFTVTKYWFYR) as a fusion peptide to the C terminus of AP internalization sequence (RQIKIWFQNRRMKWKK) (Bucci et al., 2000). Cell-permeable AP peptide was used as control as described previously (Zhu et al., 2004; Bernatchez et al., 2005). The peptides were biotinylated at the N terminus to detect their internalization in endothelial cells. We observed the internalization of both AP-CSD and AP in HPAECs by staining with rhodamine-labeled streptavidin (Fig. 1A). We also determined the relative concentration of the peptides reached inside HPAECs using SELDI-TOF MS (Fig. 1B; Table 1; see details under *Materials and Methods*). We observed the presence of 25 and 80 μM concentrations of AP peptide by incubating cells with 50 and 100 μM concentrations, respectively, in the extracellular medium for 4 h (Table 1). In the case of AP-CSD peptide, we observed the presence of 20 and 65 μM inside the cells by incubating cells with 50 and 100 μM concentrations, respectively, in the extracellular medium (Table 1). These results indicate the presence of both the AP and AP-CSD peptides inside the HPAECs. Next, we determined the effects of AP-CSD and AP on thrombin-induced increase in $[Ca^{2+}]_i$. Thrombin-induced increase in $[Ca^{2+}]_i$ was inhibited in cells incubated with AP-CSD in a dose-dependent manner compared with control cells (Fig. 1C); however, control AP had no significant effect on thrombin-induced increase in $[Ca^{2+}]_i$.(Fig. 1D). To address whether AP-CSD peptide inhibits thrombin-induced Ca^{2+} influx, HPAECs incubated with AP-CSD peptide were first stimulated with thrombin in the absence of extracellular Ca^{2+}, and then Ca^{2+} was added to the extracellular medium to assess Ca^{2+} influx. We observed that in the absence of extracellular Ca^{2+}, thrombin-induced increase in initial peak due to ER-stored Ca^{2+} depletion was markedly reduced in AP-CSD-treated cells compared with control (Fig. 2, A and B), whereas AP alone did not influence the initial peak (data not shown). Ca^{2+} influx after ER-stored Ca^{2+} depletion induced by thrombin was also significantly reduced in HPAECs exposed to AP-CSD compared with control (Fig. 2, A and B). These results demonstrate that CSD regulates

TABLE 1

Quantification of cell-permeable peptides inside HPAECs

Cell volume was determined by incubating HPAECs with [^{3}H]mannitol as described under *Materials and Methods*. A volume of 2.5 μl/10^6 cells was obtained. Cells were incubated with medium containing the indicated concentrations of peptides in a total volume of 2.46 ml/10^6 cells. The relative concentrations of peptides present in the cell extracts were calculated using mass spectra from known peptide concentrations and cell volume (see details under *Materials and Methods*). Values reported are mean of three separate experiments.

Peptide	Incubation Medium Concentration	Relative Peptide Concentration Inside the Cells
	μM	
AP	0	N.D.
AP	50	25
AP	100	80
AP-CSD	0	N.D.
AP-CSD	50	20
AP-CSD	100	65

N.D., not detectable.

both IP_3-sensitive ER-stored Ca^{2+} depletion and stored Ca^{2+} depletion-mediated Ca^{2+} influx in endothelial cells.

To characterize further the basis of inhibition of Ca^{2+} influx by the AP-CSD in HPAECs, we measured the thapsigargin-induced increase in intracellular Ca^{2+} in AP-CSD or AP-treated HPAECs. Thapsigargin-induced increase in in-

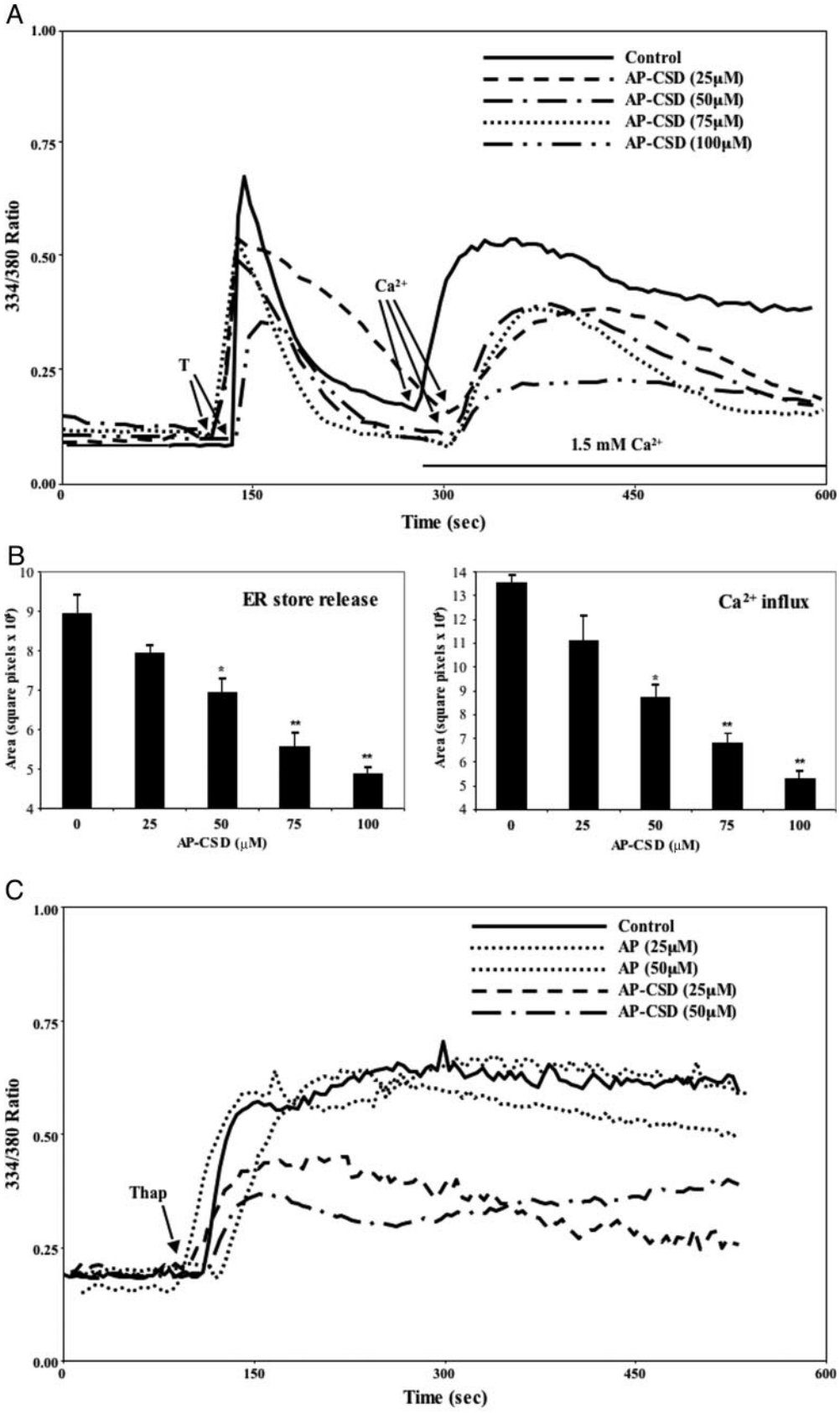

Fig. 2. A, AP-CSD peptide inhibits thrombin-induced ER-stored Ca^{2+} release and Ca^{2+} release-induced Ca^{2+} influx in HPAECs. HPAECs incubated with indicated concentrations of AP-CSD peptide were used for measuring ER-stored Ca^{2+} release and Ca^{2+} release-induced Ca^{2+} influx. After Fura 2-AM loading, cells were washed two times, placed in Ca^{2+}- and Mg^{2+}-free HBSS, and then stimulated with thrombin (50 nM). After return to baseline levels, 1.5 mM $CaCl_2$ was added to the extracellular medium to induce Ca^{2+} influx. Arrows, times at which thrombin (T) or Ca^{2+} was added. B, relative areas of initial ER-stored Ca^{2+} release and the Ca^{2+} influx peaks were compared with control and peptide-treated groups. *, $p < 0.01$; **, $p < 0.005$. C, CSD peptide inhibits thapsigargin (Thap)-induced increase in $[Ca^{2+}]_i$ in HPAECs. HPAECs incubated with the indicated concentrations of AP-CSD or AP peptides were used for measuring Thap-induced increase in $[Ca^{2+}]_i$ as described under *Materials and Methods*. Cells were placed in nominal Ca^{2+} (1.26 mM)-containing medium and then stimulated with thapsigargin (1 μM). Arrow indicates the time at which thapsigargin was added. Results shown are representative of four experiments.

tracellular Ca^{2+} was also markedly reduced in AP-CSD-incubated cells compared with AP or control cells (Fig. 2C), suggesting that CSD interacts with TRPC1 to prevent Ca^{2+} influx in HPAECs.

CSD Interacts with TRPC1 in Endothelial Cells. We have shown that TRPC1 is predominantly expressed in human vascular endothelial cells (Paria et al., 2003, 2004, 2006). Other studies have shown that the assembly of TRPC1 in a signaling complex associated with Cav-1 (Lockwich et al., 2000), and this association was necessary for SOC-mediated Ca^{2+} influx (Brazer et al., 2003). However, it is unclear whether CSD directly interacts with TRPC1 and whether this interaction is necessary for SOC-mediated Ca^{2+} influx in endothelial cells. To address this question, we incubated AP-CSD or AP with HPAECs for 4 h at 37°C, cells were washed three times with acid buffer to remove surface-bound peptides, and cells were lysed. Lysates were incubated with streptavidin-agarose beads to study the binding of TRPC1 with AP-CSD (see details under *Materials and Methods*). Streptavidin-agarose beads were washed, and bound proteins were separated on SDS-PAGE and immunoblotted with anti-TRPC1 Ab (Fig. 3A). Anti-TRPC1 Ab strongly reacted with ~85-kDa protein (TRPC1) in AP-CSD-treated cells, whereas there was a weak reaction of anti-TRPC1 Ab with TRPC1 in AP peptide-incubated cells.

To address the specificity of the interaction between CSD and TRPC1, we ectopically expressed HA-tagged CSD in HMECs, and at 48 h after transfection, cells were lysed, and lysates were immunoprecipitated with anti-HA antibody. The precipitated proteins were immunoblotted with anti-TRPC1 Ab (Fig. 3B). We observed that anti-TRPC1 Ab reacted with TRPC1 only in cell lysate from HA-tagged CSD-transfected cells but not in vector alone-transfected cells. These results indicate the interaction between TRPC1 and CSD in endothelial cells.

CSD Interacts with C Terminus of TRPC1. Previous studies have shown that binding of CSD to aromatic amino acids containing motifs ΦXΦXXXXΦ and ΦXXXXΦXXΦ, where Φ is an aromatic residue (tryptophan, phenylalanine, or tyrosine) (Couet et al., 1997). The deduced amino acid sequence of TRPC1 revealed the presence of a similar CSD binding motif in the C terminus [FRTSKYAMF (ΦXXXXΦXXΦ)]. To study the interaction between TRPC1 C-terminal peptide with CSD, we synthesized TRPC1 C-terminal peptide (residues 781–789; FRTSKYAMF) (Fig. 4A) as cell-permeable AP fusion peptide with biotin at the N terminus (AP-TRPC1-C9) (see details under *Materials and Methods*). HPAECs were incubated with AP-TRPC1-C9 for 4 h, cells were washed and lysed, and lysates were incubated with streptavidin-agarose beads (see details under *Materials and Methods*). Proteins associated with streptavidin-agarose beads were separated onto SDS-PAGE and immunoblotted with anti-Cav-1 Ab. We observed that the anti-Cav-1 Ab reacted with Cav-1 present in streptavidin-agarose-precipitated proteins from TRPC1 C-terminal peptide-incubated cells (Fig. 4B) but not from the AP sequence-incubated cells, indicating that TRPC1 C-terminal sequence (FRTSKYAMF) interacts with Cav-1 in endothelial cells.

TRPC1 C-Terminal Peptide Inhibits Thrombin-Induced Increase in Intracellular Ca^{2+} in HPAECs. We next examined the effects of cell-permeable TRPC1 C-terminal peptide on thrombin-induced increase in $[Ca^{2+}]_i$ in HPAECs. We observed that AP-TRPC1-C9 peptide pretreatment inhibited in a dose-dependent manner the thrombin-induced increase in $[Ca^{2+}]_i$ in HPAECs (Fig. 4, C and D). We also tested the effects of AP-TRPC1-C9 peptide on ER-stored Ca^{2+} release and Ca^{2+}-release activated Ca^{2+} influx in HPAECs. In this experiment, after Fura 2-AM loading, cells were stimulated with thrombin in the absence of extracellular Ca^{2+} to deplete ER-stored Ca^{2+}, and then Ca^{2+} was reapplied to assess the Ca^{2+} influx. AP-TRPC1-C9 peptide had a significant effect on Ca^{2+} release from ER (Fig. 4, E and F). In addition, AP-TRPC1-C9 peptide exposure markedly reduced the Ca^{2+} influx induced by thrombin (Fig. 4, E and F), suggesting that TRPC1-C9 peptide competes for the CSD binding domain on TRPC1.

CSD Peptide Binds to Src and Inhibits Cav-1-Tyr14 Phosphorylation in Endothelial Cells. Studies have shown that CSD interacts with signaling molecules such as Src and phosphorylates Cav-1 on Tyr14 (Minshall et al., 2000; Oh and Schnitzer, 2001; Schlegel and Lisanti, 2001; del Pozo et al., 2005); thus, we determined whether AP-CSD also interacts with Src in HPAECs. HPAECs were incubated with

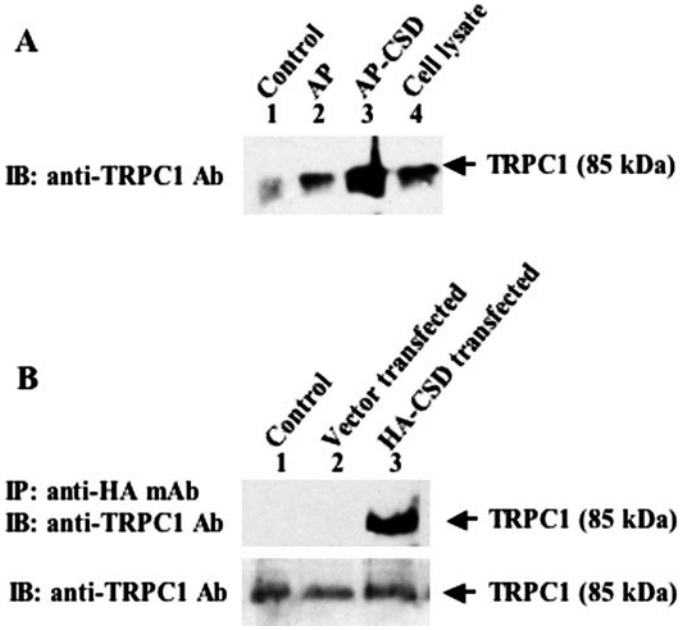

Fig. 3. A, CSD interacts with TRPC1 in endothelial cells. HPAECs incubated with 50 μM AP-CSD or AP peptide for 4 h at 37°C were washed three times with acid buffer (50 mM acetate buffer, pH 5.0, containing 0.5 M NaCl) at 4°C. Cells were lysed, and CSD binding proteins were separated using streptavidin-agarose beads pull-down (see details under *Materials and Methods*). The proteins associated with beads were separated on SDS-PAGE and immunoblotted with anti-TRPC1 antibody. The results shown are from representative experiments. The experiment was repeated three times, and the results obtained were similar. Lane 1, control; lane 2, AP peptide-incubated cells; lane 3, AP-CSD peptide-incubated cells; lane 4, cell lysate. IB, immunoblot. B, endogenous TRPC1 binds to ectopically expressed CSD domain in endothelial cells. HA-tagged CSD sequence-expressing plasmid was transfected into HMECs (see details under *Materials and Methods*). At 48 h after transfection, cell lysates were immunoprecipitated with anti-HA mAb. The precipitated proteins were separated on SDS-PAGE and immunoblotted with anti-TRPC1 polyclonal antibody. Lane 1, control; lane 2, vector-transfected control; lane 3, HA-tagged CSD sequence-expressing plasmid transfected. Anti-TRPC1 Ab reacted (85 kDa) with HA-tagged-CSD sequence-expressing cells. Cell lysates (50 μg of protein) from control, vector-transfected, and HA-tagged CSD transfected were immunoblotted with anti-TRPC1 Ab to indicate that TRPC1 expression was not altered in HMECs (bottom). IP, immunoprecipitate; IB, immunoblot.

the biotin-labeled AP-CSD or AP for 4 h, and cell lysates were used for streptavidin-agarose bead pull-down assays (see details under *Materials and Methods*). We observed binding of Src with AP-CSD peptide but not with AP-peptide (Fig. 5A), indicating that CSD interacts with Src and thus may regulate SOC function in HPAECs by this mechanism.

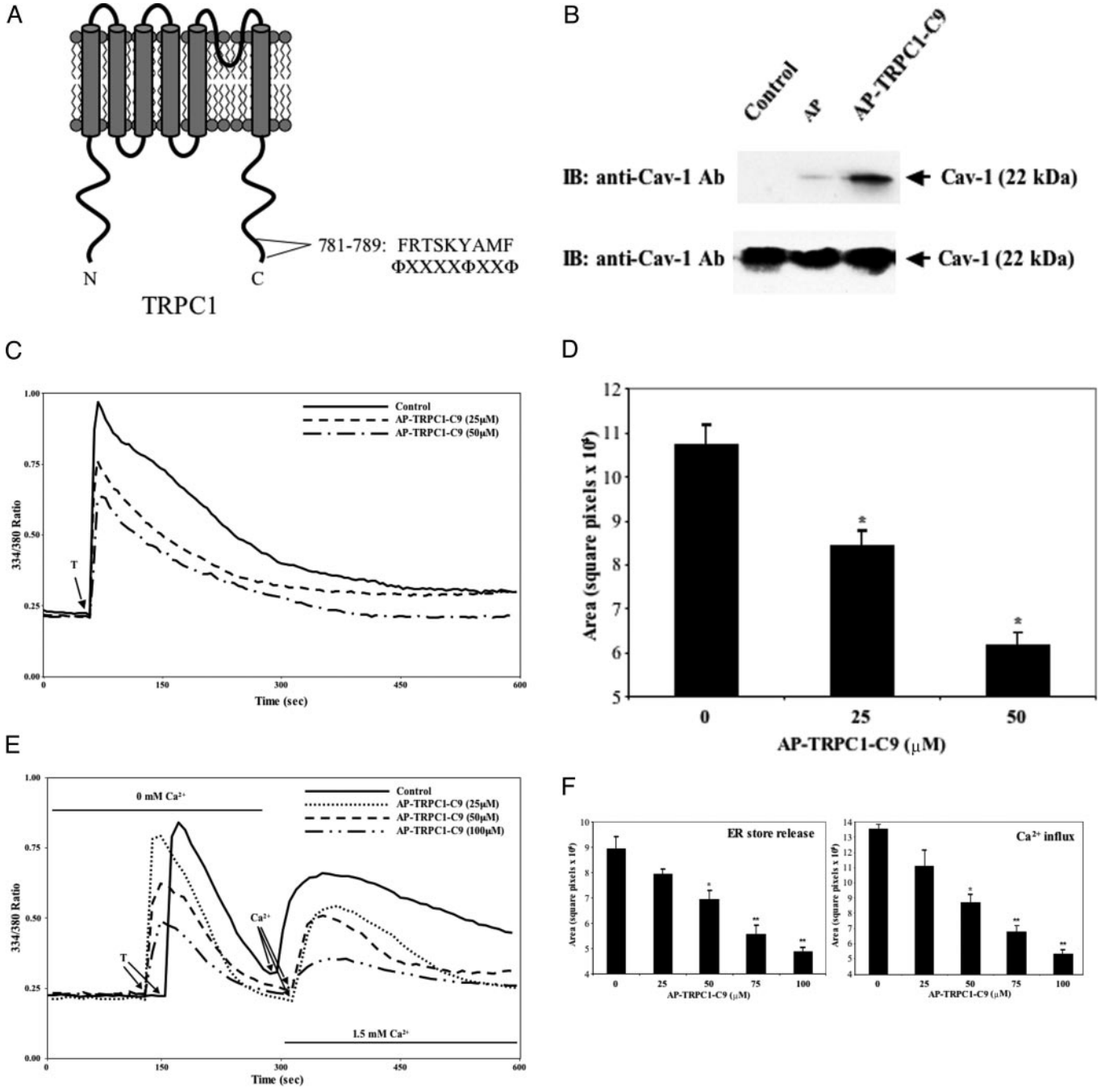

Fig. 4. Cav-1 interacts with C terminus of TRPC1. A, CSD binding consensus sequence in the C terminus of TRPC1. B, HPAECs were incubated with 25 μM concentration of either biotin-labeled AP peptide or biotin-labeled AP-TRPC1 C-terminal peptide [residues 781–789 (AP-TRPC1-C9)] for 4 h at 37°C in 1% FBS containing medium. After incubation, cell lysates were used for streptavidin-agarose pull-down (see details under *Materials and Methods*). Proteins associated with streptavidin-agarose beads were separated on SDS-PAGE and immunoblotted with anti-Cav-1 antibody (top). Lane 1, control; lane 2, AP peptide-treated cells; lane 3, AP-TRPC1-C9 peptide-treated cells. Cell lysates (20 μg of protein) from control, AP peptide, and AP-TRPC1-C9 peptide treated were immunoblotted with anti-Cav-1 Ab (bottom). C and D, TRPC1 C-terminal synthetic peptide inhibits thrombin-induced increase in $[Ca^{2+}]_i$ in HPAECs. In C, HPAECs grown to confluence were incubated with the indicated concentrations of AP-TRPC1-C9 peptide (see details under *Materials and Methods*). After incubation, cells were used for measuring thrombin-induced increase in $[Ca^{2+}]_i$ described in Fig. 1C. Arrow indicates the time at which cells were stimulated with thrombin (50 nM). Results shown are representative of four experiments. In D, relative area of peak increase in $[Ca^{2+}]_i$ after thrombin stimulation in control and AP-TRPC1-C9 peptide-treated groups were compared. *, $p < 0.01$. E and F, TRPC1 C-terminal synthetic peptide inhibits Ca^{2+} influx via TRPC1 in HPAECs. The experiment was carried out as described above in Fig. 2A. In E, after Fura 2-AM loading, cells were washed two times, placed in Ca^{2+}- and Mg^{2+}-free HBSS, and stimulated with thrombin (50 nM). After return to baseline levels, 1.5 mM $CaCl_2$ was added to the extracellular medium to induce Ca^{2+} influx. Arrows, times at which thrombin (T) or Ca^{2+} was added. Results shown are representative of four experiments. In F, relative area of initial ER-stored Ca^{2+} release and the Ca^{2+} influx peaks were compared with the control and the AP-TRPC1-C9 peptide-treated cells. *, $p < 0.01$; **, $p < 0.005$.

Studies have shown that Src-mediated Cav-1 phosphorylation on Tyr14 is crucial in signal-transduction events in caveolae (Shajahan et al., 2004; del Pozo et al., 2005); thus, we determined the possibility that CSD peptide inhibits Cav-1 phosphorylation on Tyr14 in HPAECs and interferes with SOC-mediated Ca^{2+} influx. HPAECs were incubated with either AP-CSD or AP and challenged with thrombin, and cell lysates were immunoblotted with anti-phospho-Tyr14 Cav-1-specific antibody. In control cells (i.e., in absence of thrombin stimulation), we observed Cav-1 phosphorylation on Tyr14; however, phosphorylation was further increased on thrombin stimulation. Maximum phosphorylation was seen at 2 min after thrombin challenge, and it returned to baseline at 10 min (Fig. 5B). Treatment of cells with AP-CSD at a concentration less than 25 μM prevented both basal and thrombin-induced Tyr14 phosphorylation of Cav-1, whereas the control peptide (AP peptide) had no effect (Fig. 5B).

Coexpression of Cav-1 and TRPC1 Inhibits Thrombin-Induced Increase in $[Ca^{2+}]_i$ in Endothelial Cells. We have shown that increased SOC-mediated Ca^{2+} influx occurs in TRPC1 overexpressing endothelial cells (Paria et al., 2004); thus, we investigated the effects of Cav-1 overexpression on TRPC1-mediated Ca^{2+} influx in endothelial cells. We ectopically expressed Myc-TRPC1, Myc-TRPC1 plus WT-Cav-1, or Myc-TRPC1 plus Cav-1-14F mutant in HMECs. Expression levels of Myc-TRPC1, WT-Cav-1, and Cav-1-14F mutant were determined by immunoblotting transfected HMEC lysates with anti-Myc mAb and anti-Cav-1 Ab (Fig. 5C). Thrombin produced a 2-fold increase in $[Ca^{2+}]_i$ in Myc-TRPC1-expressing HMECs compared with control (vector alone-transfected) cells (Fig. 5, D and E). Coexpression of WT-Cav-1 with Myc-TRPC1 reduced the thrombin-induced increase in $[Ca^{2+}]_i$ in HMECs. In addition, coexpression of phosphorylation-defective Cav-1 mutant (Cav-1-14F) with

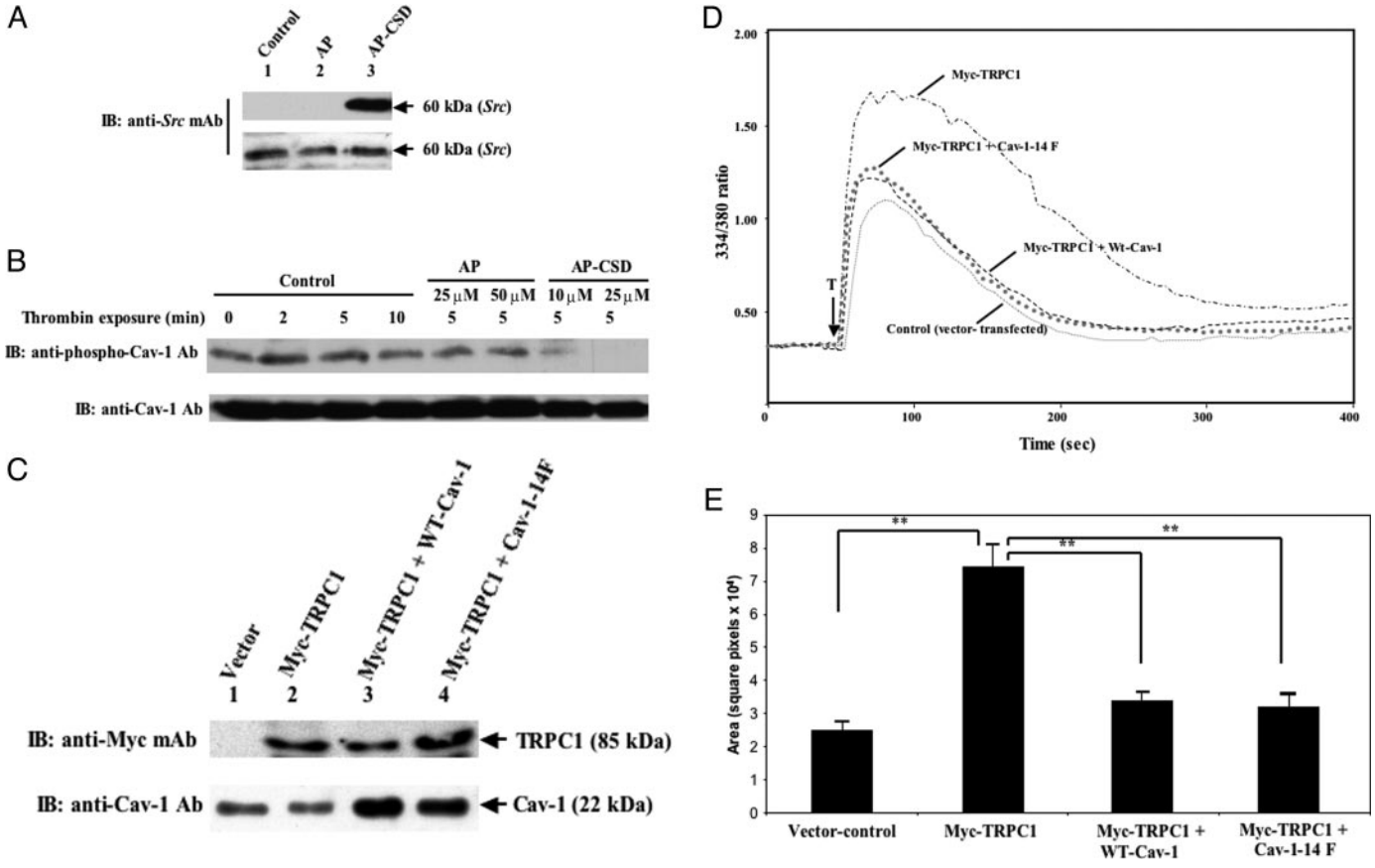

Fig. 5. A, Cav-1 scaffolding sequence interacts with Src in HPAECs. HPAECs grown to confluence on culture dishes were incubated with either AP peptide or AP-CSD peptide in 1% FBS containing medium for 4 h at 37°C. After this incubation period, cells were washed, lysed, and lysates were used for streptavidin-agarose beads pull-down (see details under *Materials and Methods*). Proteins associated with streptavidin-agarose beads were separated on SDS-PAGE and immunoblotted with anti-Src mAb. The results shown are from representative experiments. The experiment was repeated three times, and the results obtained were similar. Cell lysates (50 μg of protein) from control, AP peptide, and AP-CSD peptide-treated were immunoblotted with anti-Src mAb (bottom). B, CSD peptide inhibits Cav-1 phosphorylation on Tyr14 in endothelial cells. HPAECs grown to confluence on culture dishes were incubated with either AP peptide or AP-CSD peptide (see details under *Materials and Methods*). After incubation, cells were washed and incubated in serum-free medium for 2 h, and cells were stimulated with thrombin (50 nM) for the indicated times. After thrombin treatment, cells were placed on ice, washed three times at 4°C, lysed, the lysate proteins were separated on SDS-PAGE, and Src activation-dependent Cav-1 phosphorylation was detected by immunoblotting with anti-phospho-Tyr14 Cav-1 antibody. The results shown are from representative experiments. The experiment was repeated three times, and the results obtained were similar. C–E, Cav-1 coexpression with TRPC1 prevents Ca^{2+} influx via SOC in endothelial cells. HMECs grown to 60 to 70% confluence were transfected with Myc-TRPC1 expression plasmid (1 μg/ml) alone or cotransfected with either WT-Cav-1 (1 μg/ml) or Cav-1-14F mutant (1 μg/ml) expression constructs using LipofectAMINE Plus reagents (Ellis et al., 1999). In C, after transfection, cells were lysed and immunoblotted with either anti-Myc-mAb (to determine TRPC1 expression) or anti-Cav-1 Ab. In D, at 48 h after transfection, cells were used for measuring cytosolic Ca^{2+} (see details under *Materials and Methods*). After fura-2 loading, cells were placed in nominal Ca^{2+} (1.26 mM)-containing medium and then stimulated with thrombin (50 nM). Arrow indicates the time at which thrombin (T) was added. Results shown are representative of four experiments. In E, the relative area of peak increase in $[Ca^{2+}]_i$ after thrombin stimulation in control (vector-transfected) and transfected cells were compared. **, $p < 0.005$.

Myc-TRPC1 resulted in the same reduction in thrombin-induced increase in $[Ca^{2+}]_i$. Thus, Cav-1 may regulate SOC function by directly binding to TRPC1, and Cav-1 phosphorylation on Tyr14 does not seem to be required for Ca^{2+} entry via SOC.

Discussion

Ca^{2+} entry in nonexcitable cells via SOCs regulates many signaling events, including gene expression, cell survival, and cell death (Putney, 1999; Nilius and Droogmans, 2001; Montell et al., 2002; Birnbaumer et al., 2003). We have shown that Ca^{2+} entry via SOC in endothelial cells is crucial in regulating vessel wall barrier function (Tiruppathi et al., 2003). Our studies (Paria et al., 2003, 2004, 2006) and others (Groschner et al., 1998; Brough et al., 2001) have demonstrated that TRPC1 expressed in human vascular endothelial cells is an essential component of SOC. TRPC1 can be activated by the $G_{\alpha q/11}$-linked phospholipase C pathway (Nilius and Droogmans, 2001; Tiruppathi et al., 2003). However, the molecular mechanism of Ca^{2+} influx through TRPC1 is not well understood. Brazer et al. (2003) showed the specific binding of Cav-1 with N and C termini of TRPC1 in human submandibular gland cells. They also showed that interaction between Cav-1 and TRPC1 was essential for the membrane localization of TRPC1 and that Cav-1 N terminus domain (residues 51–169) binding to TRPC1 was involved in regulating Ca^{2+} influx through TRPC1. However, it is known that Cav-1 N terminus contains a scaffolding domain [i.e., residues 82–101 (CSD)], which regulates key signaling events. For example, binding of eNOS to CSD prevented NOS activation in endothelial cells (Bucci et al., 2000). In addition, Ca^{2+} influx through SOC was shown to disrupt the eNOS interaction with CSD and thus facilitated the binding of eNOS to the Ca^{2+}/calmodulin complex required for activation of eNOS (Michel et al., 1997). Because CSD is localized in the N terminus of Cav-1, in the present study we addressed the possible role of CSD in regulating store-operated Ca^{2+} influx in endothelial cells. We observed that the cell-permeable CSD peptide inhibited thrombin-induced ER-stored Ca^{2+} release and stored Ca^{2+} release-induced Ca^{2+} influx. CSD peptide also suppressed the thapsigargin-induced Ca^{2+} entry, suggesting that CSD may directly interact with TRPC1 to regulate the Ca^{2+} influx via SOC. Furthermore, we observed the specific binding of CSD to TRPC1 using the cell-permeable AP-CSD peptide and ectopically expressed CSD sequence. Together, these findings suggest that the interaction between TRPC1 and CSD is crucial in regulating Ca^{2+} influx via SOC in endothelial cells.

Couet et al. (1997) recently identified CSD binding motif on $G_{i2}\alpha$ protein using phage display libraries. They showed that CSD sequence interacts with aromatic amino acid-containing motifs ΦXΦXXXXΦ and ΦXXXXΦXXΦ, where Φ is an aromatic residue (tryptophan, phenylalanine, or tyrosine). We noted that the deduced amino acid sequence of TRPC1 had a similar CSD binding motif in the C terminus [FRTSKYAMF (ΦXXXXΦXXΦ)]. Thus, we used the CSD binding motif sequence present in the TRPC1 C terminus (FRTSKYAMF, TRPC1-C9 peptide) to study its effects on Ca^{2+} influx via SOC. Incubation of HPAECs with AP-TRPC1-C9 peptide was shown to inhibit the stored Ca^{2+} release-activated Ca^{2+} influx in HPAECs. We also observed specific binding of AP-TRPC1-C9 peptide to Cav-1, indicating that TRPC1 interaction with Cav-1 is required for Ca^{2+} influx via SOC.

Caveolae have been shown to form mobile-signaling platforms by sequestering multiple signaling proteins that bind to CSD (Schlegel and Lisanti, 2001). Using Indo-1 and a confocal laser scanning system, Isshiki et al. (1998) identified that Ca^{2+} waves preferentially occurred in the Cav-1-rich cell edges in response to shear stress or ATP in bovine aortic endothelial cells. They also demonstrated by engineering Ca^{2+}-sensing yellow chameleon targeted to caveolae that Ca^{2+} influx in response to ER-stored depletion occurred preferentially in caveolae (Isshiki et al., 2002). Ca^{2+} influx in endothelial caveolae was markedly reduced by disturbing the caveolae structure with methyl-β-cyclodextrin (Bergdahl et al., 2003). Other studies have shown the interaction between SOC (i.e., TRP channels) and IP_3 receptors (Boulay et al., 1999; Brownlow et al., 2004) was associated with the caveolae-signaling complex (Lockwich et al., 2000; Isshiki and Anderson, 2003). As we observed the inhibition of thrombin-induced ER-stored Ca^{2+} release by both cell-permeable AP-CSD and AP-TRPC1-C9 peptides in HPAECs suggest that these peptides may be interfering in the assembly of signaling complex in the caveolae and thus may affect the ER-associated IP_3 receptor function in endothelial cells.

Cav-1 is known to be abundantly expressed in endothelial cells (Minshall et al., 2000; Oh and Schnitzer, 2001), thus making it an important determinant of Ca^{2+} signaling in these cells. Overexpression of Cav-1 in endothelial cells was shown to impair caveolae-mediated signaling events in endothelial cells (Minshall et al., 2000). We have shown that Src family tyrosine kinase, by promoting Tyr14 phosphorylation of Cav-1, regulated a crucial function of caveolae in endothelial cells, caveolae-mediated endocytosis (Tiruppathi et al., 1997; Minshall et al., 2000; Shajahan et al., 2004). In the present study, we observed that both basal and thrombin-induced Tyr14 phosphorylation of Cav-1 were prevented by the cell-permeable CSD peptide. CSD peptide concentration at 10 μM prevented thrombin-induced Tyr14 phosphorylation on Cav-1, whereas this concentration had no significant effect on either ER-stored Ca^{2+} release or Ca^{2+} influx in HPAECs. This finding suggests that Tyr14 phosphorylation on Cav-1 is apparently not required for Ca^{2+} influx via SOC. We also cotransfected WT-Cav-1 or Cav-1-14F mutant with TRPC1 cDNA in an endothelial cell line (HMECs), and measured thrombin-induced increase in $[Ca^{2+}]_i$. TRPC1 expression alone increased thrombin-induced increase in $[Ca^{2+}]_i$, whereas coexpression of either WT-Cav-1 or Cav-1-14F mutant with TRPC1 prevented the increase in $[Ca^{2+}]_i$, indicating that Cav-1 binding to TRPC1 is more important in regulating SOC function in endothelial cells than Cav-1 phosphorylation on Tyr14.

In summary, we showed that the cell-permeable CSD peptide inhibited thrombin-induced ER-stored Ca^{2+} release, and stored Ca^{2+} release activated Ca^{2+} influx in human vascular endothelial cells. We identified the CSD docking sequence on TRPC1 C-terminal region as being crucial in regulating Ca^{2+} signaling via SOC in endothelial cells. In addition, we showed that binding of CSD peptide to key molecules is required for the activation of TRPC1-mediated Ca^{2+} signaling pathways. Thus, the interaction of CSD with TRPC1 plays an important role in the mechanism of store-operated Ca^{2+} influx and thereby may regulate endothelial function.

References

Bergdahl A, Gomez MF, Dreja K, Xu SZ, Adner M, Beech DJ, Broman J, Hellstrand P, and Sward K (2003) Cholesterol depletion impairs vascular reactivity to endothelin-1 by reducing store-operated Ca^{2+} entry dependent on TRPC1. *Circ Res* **93:**839–847.

Bernatchez PN, Bauer PM, Yu J, Prendergast JS, He P, and Sessa WC (2005) Dissecting the molecular control of endothelial NO synthase by caveolin-1 using cell-permeable peptides. *Proc Natl Acad Sci USA* **102:**761–766.

Birnbaumer L, Yidirim E, and Abramowitz J (2003) A comparison of the genes coding for canonical TRP channels and their M, V and P relatives. *Cell Calcium* **33:**419–432.

Boulay G, Brown DM, Qin N, Jiang M, Dietrich A, Zhu MX, Chen Z, Birnbaumer M, Mikoshiba K, and Birnbaumer L (1999) Modulation of Ca^{2+} entry by polypeptides of the inositol 1,4, 5-trisphosphate receptor (IP3R) that bind transient receptor potential (TRP): evidence for roles of TRP and IP3R in store depletion-activated Ca^{2+} entry. *Proc Natl Acad Sci USA* **96:**14955–14960.

Brazer SC, Singh BB, Liu X, Swaim W, and Ambudkar IS (2003) Caveolin-1 contributes to assembly of store-operated Ca^{2+} influx channels by regulating plasma membrane localization of TRPC1. *J Biol Chem* **278:**27208–27215.

Brough GH, WU S, Cioffi D, Moore TM, Li M, Dean N, and Stevens T (2001) Contribution of endogenously expressed Trp1 to a Ca^{2+}-selective, store-operated Ca^{2+} entry pathway. *FASEB J* **15:**1727–1738.

Brownlow SL, Harper AGS, Harper MT, and Sage SO (2004) A role for hTRPC1 and lipid raft domains in store-mediated calcium entry in human platelets. *Cell Calcium* **35:**107–113.

Bucci M, Gratton JP, Rudic RD, Acevedo L, Roviezzo F, Cirino G, and Sessa WC (2000) In vivo delivery of the caveolin-1 scaffolding domain inhibits nitric oxide synthesis and reduces inflammation. *Nat Med* **6:**1362–1367.

Cool DR and Hardiman A (2004) C-Terminal sequencing of peptide hormones using carboxypeptidase Y and SELDI-TOF mass spectrometry. *Biotechniques* **36:**32–34.

Couet J, Li S, Okamoto T, Ikezu T, and Lisanti MP (1997) Identification of peptide and protein ligands for the caveolin-scaffolding domain. Implications for the interaction of caveolin with caveolae-associated proteins. *J Biol Chem* **272:**6525–6533.

del Pozo MA, Balasubramanian N, Alderson NB, Kiosses WB Grande-Garcia A, Anderson RGW, and Schwartz MA (2005) Phospho-caveolin-1 mediates intergrin-regulated membrane domain internalization. *Nat Cell Biol* **7:**901–908.

Dietrich A, Mederos Y, Schnitzler M, Emmel J, Kalwa H, Hofmann T, and Gudermann T (2003) N-linked protein glycosylation is a major determinant for basal TRPC3 and TRPC6 channel activity. *J Biol Chem* **278:**47842–47852.

Drab M, Verkade P, Elger M, Kasper M, Lohn M, Lauterbach B, Menne J, Lindschau C, Mende F, Luft FC, et al. (2001) Loss of caveolae, vascular dysfunction, and pulmonary defects in caveolin-1 gene-disrupted mice. *Science (Wash DC)* **293:**2449–2452.

Ellis CA, Malik AB, Gilchrist A, Hamm H, Sandoval, Voyno-Yaseketskaya T, and Tiruppathi C (1999) Thrombin induces proteinase-activated receptor-1 gene expression in endothelial cells via activation of Gi-linked ras/mitogen-activated protein kinase pathway. *J Biol Chem* **274:**13718–13727.

Freichel M, Suh SH, Pfeifer A, Schweig U, Trost C, Weissgerber P, Biel M, Philipp S, Freise D, Droogmans G, et al. (2001) Lack of an endothelial store-operated Ca^{2+} current impairs agonist-dependent vasorelaxation in TRP4−/− mice. *Nat Cell Biol* **3:**121–127.

Groschner K, Hingel S, Lintschinger B, Balzer M, Romanin C, Zhu X, and Schreibmayer W (1998) Trp proteins form store-operated cation channels in human vascular endothelial cells. *FEBS Lett* **437:**101–106.

Hardiman A, Friedman TC, Grunwald WC Jr, Furuta M, Zhu Z, Steiner DF, and Cool DR (2005) Endocrinomic profile of neurointermediate lobe pituitary prohormone processing in PC1/3- and PC2-null mice using SELDI-TOF mass spectrometry. *J Mol Endocrinol* **34:**739–751.

Isshiki M and Anderson RGW (2003) Function of caveolae in Ca^{2+} entry and Ca^{2+}-dependent signal transduction. *Traffic* **4:**717–723.

Isshiki M, Ando J, Korenaga R, Kogo H, Fujimoto T, Fujita T, and Kamiya A (1998) Endothelial Ca^{2+} waves preferentially originate at specific loci in caveolin-rich cell edges**.** *Proc Natl Acad Sci USA* **95:**5009–5014.

Isshiki M, Ying YS, Fujita T, and Anderson RGW (2002) A molecular sensor detects signal transduction from caveolae in living cells. *J Biol Chem* **277:**43389–43398.

Liu X, Wang W, Sing BB, Lockwich T, Jadlowiec J, O'Connel B, Wellner R, Zhu MX, and Ambudkar IS (2000) Trp1, a candidate protein for the store-operated Ca^{2+} influx mechanism in salivary gland cells. *J Biol Chem* **275:**3403–3411.

Lockwich TP, Liu X, Singh BB, Jadlowiec J, Weiland S, and Ambudkar IS (2000) Assembly of Trp1 in a signaling complex associated with caveolin-scaffolding lipid raft domains. *J Biol Chem* **275:**11934–11942.

Michel JB, Feron O, Sacks D, and Michel T (1997) Reciprocal regulation of endothelial nitric-oxide synthase by Ca^{2+}-calmodulin and caveolin. *J Biol Chem* **272:**15583–15586.

Minshall RD, Tiruppathi C, Vogel SM, Niles WD, Gilchrist A, Hamm HE, and Malik AB (2000) Endothelial cell-surface gp60 activates vesicle formation and trafficking via G_i-coupled Src kinase signaling pathway. *J Cell Biol* **150:**1057–1070.

Montell C, Birnbaumer L, and Flockerzi V (2002) The TRP channels, a remarkably functional family. *Cell* **108:**595–598.

Nilius B and Droogmans G (2001) Ion channels and their functional role in vascular endothelium. *Physiol Rev* **81:**1415–1459.

Oh P and Schnitzer JE (2001) Segregation of heterotrimeric G proteins in cell surface microdomains. G_q binds caveolin to concentrate in caveolae, whereas G_i and G_s target lipid rafts by default. *Mol Biol Cell* **12:**685–698.

Paria BC, Bair AM, Xue J, Yu Y, Malik AB, and Tiruppathi C (2006) Ca^{2+} influx-induced by PAR-1 activates a feed-forward mechanism of TRPC1 expression via NF-kappa B activation in endothelial cells. *J Biol Chem* **281:**20715–20727.

Paria BC, Malik AB, Kwiatek AM, Rahman A, May MJ, Ghosh S, and Tiruppathi C (2003) Tumor necrosis factor-alpha induces nuclear factor-κB-dependent TRPC1 expression in endothelial cells. *J Biol Chem* **278:**37195–37203.

Paria PC, Vogel SM, Ahmmed GU, Alamgir S, Shroff J, Malik AB, and Tiruppathi C (2004) Tumor necrosis factor-α-induced TRPC1 expression amplifies store-operated Ca^{2+} influx and endothelial permeability. *Am J Physiol* **287:**L1303–L1313.

Pedersen SF, Owsianik G, and Nilius B (2005) TRP channels: an overview. *Cell Calcium* **38:**233–252.

Putney JW Jr (1999) TRP, inositol 1,4,5-triphosphate receptors, and capacitative calcium entry. *Proc Natl Acad Sci USA* **96:**14669–14671.

Sandoval R, Malik AB, Minshall RD, Kouklis P, Ellis CA, and Tiruppathi C (2001a) Ca^{2+} signaling and PKCα activate increased endothelial permeability by disassembly of VE-cadherin junctions. *J Physiol (Lond)* **533:**433–435.

Sandoval R, Malik AB, Naqvi T, Mehta D, and Tiruppathi C (2001b) Requirement of Ca^{2+} signaling in the mechanism of thrombin-induced increase in endothelial permeability. *Am J Physiol* **280:**L239–L247.

Schlegel A and Lisanti MP (2001) Caveolae and their coat proteins, the caveolins: from electron microscopic novelty to biological launching pad. *J Cell Physiol* **186:**329–337.

Shajahan AN, Sverdlov M, Hirth AM, Timblin BK, Tiruppathi C, Malik AB, and Minshall RD (2004) *Src*-dependent caveolin-1 phosphorylation destabilizes caveolin-1 oligomers and activates vesicle fission in endothelial cells. *Mol Biol Cell* **15:**330a.

Tiruppathi C, Freichel M, Vogel SM, Paria BC, Mehta D, Flockerzi V, and Malik AB (2002) Impairment of store-operated Ca^{2+} entry in $TRPC4^{-/-}$ mice interferes with increase in lung microvascular permeability. *Circ Res* **91:**70–76.

Tiruppathi C, Minshall RD, Paria BC, Vogel SM, and Malik AB (2003) Role of Ca^{2+} signaling in the regulation of endothelial permeability. *Vascul Pharmacol* **39:**173–185.

Tiruppathi C, Song W, Bergenfeldt M, Sass P, and Malik AB (1997) Gp60 activation mediates albumin transcytosis in endothelial cells by tyrosine kinase-dependent pathway. *J Biol Chem* **272:**25968–25975.

Zhu L, Schwegler-Berry D, Castranova V, and He P (2004) Internalization of caveolin-1 scaffolding domain facilitated by *Antennapedia* homeodomain attenuates PAF-induced increase in microvessel permeability. *Am J Physiol* **286:**H195–H201.

Address correspondence to: Dr. Chinnaswamy Tiruppathi, Department of Pharmacology (M/C868), College of Medicine, University of Illinois at Chicago, 835 S. Wolcott Avenue, Chicago, IL 60612. E-mail: tiruc@uic.edu